Design and optimization of patient-specific, 3D printed pediatric laryngoscopes

R. Sims[1], M. Boutelle[1], J. Inziello[1], and F. Lobo Fenoglietto, J. Stubbs[1*]

[1] *PD3D Lab, University of Central Florida, Orlando, United States of America*
[*] *Corresponding author, email: jstubbs@ist.ucf.edu*

Abstract: Laryngoscopes have been used for endotracheal intubation since the early 1900s. Macintosh and Miller blade designs are the most widely accepted with recent improvements, including embedded optics focused on addressing challenging airways. Patient-specific 3-D Printed laryngoscope blades offer a valuable approach to difficult airway intubation. Our team introduces a proof-of-concept approach to using Imaging (CT and MRI) data to design a patient-specific laryngoscope blade.

I. Introduction

In 1911, Dr. Chevalier Jackson developed the first laryngoscope that allowed for the insertion of an endotracheal tube (ETT) [1]. Modern laryngoscopes, such as the Macintosh and Miller, began manufacturing in the early 1940's [2]. In the last few decades, laryngoscope design changes have focused on addressing challenging airways. Most modern laryngoscopes, such as the McGrath, Glidescope and Airtraq, feature integrated optics and video screens. Additionally, the three brands also feature variable-size, single-use (disposable) blades. Blade sizes are distributed unevenly across adults (3-4 sizes), pediatrics (one size), and neonates (one size). Sizes match a range of ETT sizes (2.5-3.5 for neonate, and 4.0-5.5 for pediatrics) [3]. This is relevant to pediatric and neonatal cases, in which size options are limited.

Difficulties with intubation represent the main cause of pediatric, anesthesia-related morbidities and mortality [4]. Patient-specific blades could provide safer and more reliable intubation in the case of normal and abnormal airways. 3D printing can enable a rapid and cost-effective fabrication of multi-material patient specific blades.

The development of patient specific devices requires the integration of advanced Image reconstruction, design, and manufacturing technologies. Using SideFX's Houdini, we have consolidated the reconstruction and design processes into a single program.

II. Material and methods

II.I. Patient data

De-identified CT DICOM datasets from three pediatric cases were obtained from Nemours Children's Hospital (Lake Nona, FL, USA). In addition to age, retrieved information pertained solely to findings that could influence the patient's airway. The first patient, 18 months old, did not present any lesions or abnormalities affecting the airway. The second patient, 2 mo., presented a lesion deep to the left lobe of thyroid gland and medial to the left common carotid artery. The third patient, 18 mo., presented a lesion on the right side of the neck. The lesion compromised the patient's oral cavity, oropharynx, and nasopharynx.

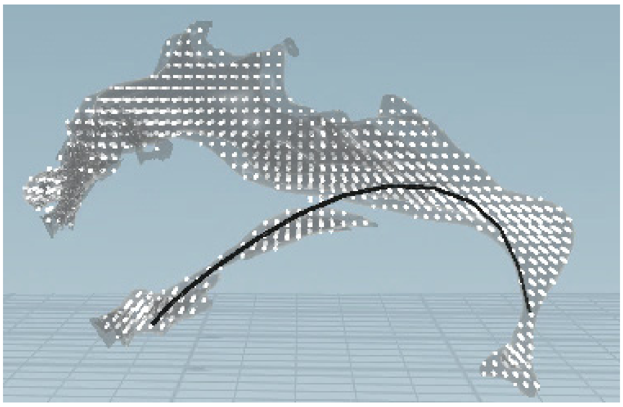

Figure 1: Space colonization algorithms use a reference point cloud and a starting point to generate a path. Point clouds were generated from each patient's airway geometry.

II.II. Houdini Program

Houdini from SideFX is a motion graphics procedural system develop primarily for the gaming and Film industry. Relying on Houdini's Python 2.x compatibility and Pydicom, our team built custom functions to: (1) Import DICOM dataset into a voxel (3D pixel) volume, (2) Map the associated Hounsfield data to a [0, 1] density scale, (3) Pad boundary voxel data, and (4) generate a closed geometry, segmentation, or 3D reconstruction of the patient's anatomy.

Surface artifacts were removed from the 3D reconstruction using voxel-based erosions. A copy of the reconstruction was then dilated until internal anatomical features were filled. The dilated copy was then projected onto the original reconstruction, in a process referred to as shrink-wrapping. The patient's airway geometry was extracted through a Boolean subtraction between the original reconstruction and the projected copy.

Space colonization algorithms (SCA) generated build paths that conformed to each patient's airway [5]. SCAs require a reference point cloud and a starting point for path generation. Point clouds were generated from each patient's airway geometry. The mouth of each patient was manually chosen as the starting point. SCAs were force stop after reaching the vicinity of each patient's epiglottis. The resulting path was used to extrude a cross-section of a laryngoscope blade. The geometry was exported as a

DOI: 10.18416/AMMM.2019.1909S01T01

surface file (.OBJ) for further editing and fabrication (Figure 1).

III. Results and discussion

Closed geometries were segmented with a fixed threshold value of 0.20. This value represented 20% of the DICOM's native HU scale. Minimal deviations were expected due to the sharp density contrast between air and tissue.

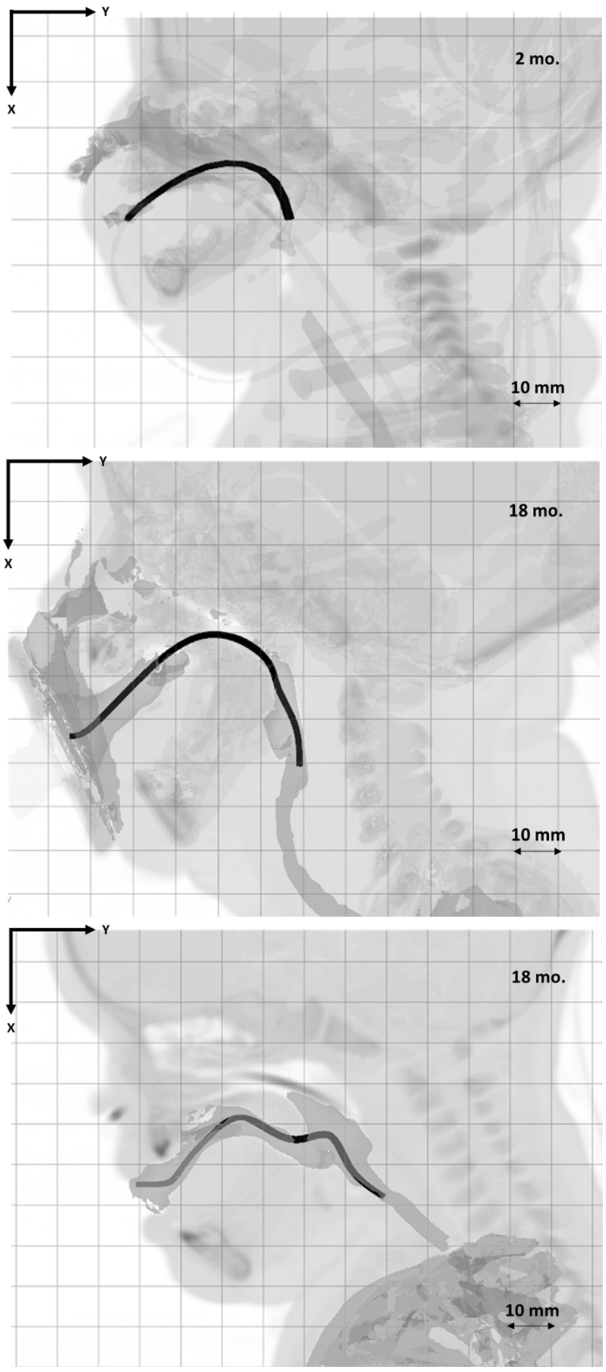

Figure 2: CT sagittal cross-section with overlaid, corresponding patient-specific laryngoscope blade

Reconstruction detail, given by the voxel resolution, varied in accordance to the patient's age and size. A resolution of 0.1 mm/voxel was required to preserve the features from the 2 mo. patient. In contrast, a resolution of 0.8 mm/voxel was used for the 18 mo. Patients.

Voxel-based erosions and dilations influenced the shrink wrapping process, which ultimately benefited from a smooth and enlarged copy of the reconstructed geometry. Reconstructed geometries were eroded by ≈2.4 mm, enough to remove surface artifacts. Surface artifacts consisted of feeding and respiratory tubes, leads, etc. The Copied of the reconstructions were dilated by ≈8.0 mm, enough to fill internal structures or features.

Point clouds, derived from the patient's airway geometry, were defined by a point separation parameter. Much like voxel resolution, point separation was affected by the size of the patient. The airway point cloud of the 2 mo. patient featured a 1 mm point separation. In contrast, a 3 mm point separation sufficed for the 18 mo. Patients. Size difference also influenced the number of steps taken by the space colonization algorithm. Solving the path for the 2 mo. patient only required 6 steps (or frames), while 10 steps were needed for both 18 mo. patients.

Finally, three patient-specific prototype laryngoscope blades were extruded using the calculated airway path. Overlays of the extruded blades and a sagittal cross-section of the patient's CT are used to depict the results (Figure 2).

IV. Conclusions

The present work described a proof-of-concept method for the design of a patient-specific laryngoscope blade. Our results show that, although tuning and validation are necessary, it is feasible to consolidate the processes of reconstruction and design in a single program. Future work will be focused on expanding patient data population, further constraining and automating sub-processes, and outlining validation experiments.

AUTHOR'S STATEMENT

The research related to human use complies with all the relevant national regulations, institutional policies and was performed in accordance with the tenets of the Helsinki Declaration, and has been approved by the authors' institutional review board or equivalent committee.

REFERENCES

[1] Christopher M. Burkle, Fernando A. Zepeda, Douglas R. Bacon, Steven H. Rose; A Historical Perspective on Use of the Laryngoscope as a Tool in Anesthesiology. Anesthesiology 2004;100(4):1003-1006.

[2] Amornyotin, S., Prakanrattana, U., Vichitvejpaisal, P., Vallisut, T., Kunanont, N., & Permpholprasert, L. (2010). Comparison of the clinical use of macintosh and miller laryngoscopes for orotracheal intubation by second-month nurse students in anesthesiology. Anesthesiology research and practice, 2010, 432846. doi:10.1155/2010/432846

[3] Savoldelli, G. L., Schiffer, E. , Abegg, C. , Baeriswyl, V. , Clergue, F. and Waeber, J. L. (2008), Comparison of the Glidescope®, the McGrath®, the Airtraq® and the Macintosh laryngoscopes in simulated difficult airways*. Anaesthesia, 63: 1358-1364. doi:10.1111/j.1365-2044.2008.05653.x

[4] M. Weiss and T. Engelhardt, "Proposal for the management of the unexpected difficult pediatric airway," Pediatric Anesthesia, no. 20, pp. 454-464, 2010.

[5] Runions, A., Lane, B. and Prusinkiewicz P., "Modeling Trees with a Space Colonization Algorithm," Eurographics Workshop on Natural Phenomena, 2007.